

Supplementary Results for Funny-Valen-Tine: Planning Solution Distribution Enhances Machine Abstract Reasoning Ability

Ruizhuo Song, Member, IEEE, Beiming Yuan

A. Ablation study

In this section, we conduct an ablation study on the three regression tasks introduced by the Funny method. The ablation experiment will be conducted on the PGM database. Specifically, we first remove all the regression tasks, and the Valen method combined with Funny degrades to a form as shown in the Figure 1. As can be seen from the figure 1, at this point, Valen is essentially equivalent to the ordinary Valen with the exception of adding Gaussian noise ϵ to the extracted multi-view representations. The results of this ablation experiment are recorded in the “Funny 1+Valen” entry of Table I.

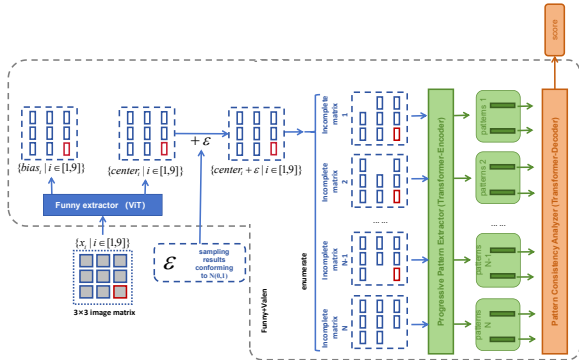


Fig. 1. Funny 1+Valen

Based on the previous experiment, we reintroduce the regression tasks indicated by the green dashed line and yellow dashed line in Funny, which results in the combination of Funny and Valen having the structure depicted in the Figure 2. The results achieved by this configuration of Funny on the PGM are recorded in the “Funny 2+Valen” entry of Table I.

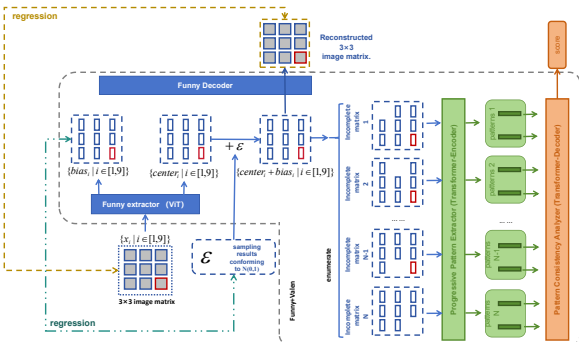


Fig. 2. Funny 2+Valen

Subsequently, based on the first ablation experiment, we reinstated the regression tasks indicated by the green dashed line and red dashed line in Funny. The structure after reinstatement can be seen in Figure 3. The results of this ablation experiment are recorded in the “Funny3+Valen” entry of Table I.

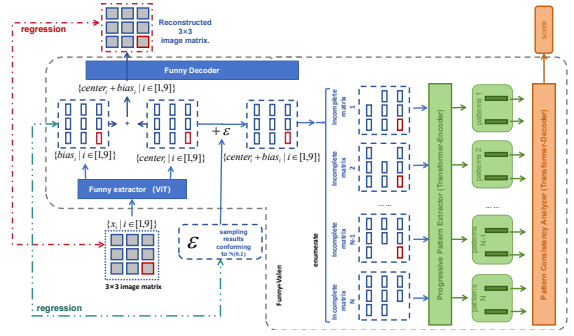


Fig. 3. Funny 3+Valen

It is worth mentioning that we conducted ablation experiments by replacing the Half-Split Decoder in the Funny method with the inverted version of the ViT, and documented the corresponding results in Table I under the entry “Funny (normal decoder) + Valen”. Additionally, we further substituted the Half-Split Decoder in two subsequent ablation studies labeled “Funny2+Valen” and “Funny3+Valen”. The outcomes of these extended ablation experiments are reported in Table I, specifically under the headings “Funny2 (normal decoder) + Valen” and “Funny3 (normal decoder) + Valen”, respectively.

TABLE I
REASONING ACCURACIES OF MODELS ON PGM.

Model	Test Accuracy(%)
Valen	98.5
Valen+Tine	98.8
Funny+Valen	99.0
Funny 1+Valen	98.7
Funny 2+Valen	98.3
Funny 3+Valen	98.3
Funny(normal decoder)+Valen	98.4
Funny 2(normal decoder)+Valen	97.9
Funny 3(normal decoder)+Valen	97.8

B. The interpretability brought by the SBR method for Valen

SBR has planned the distribution of $\{P_{nm}|n \in [1, 9], m \in [1, M]\}_{v=1}^V$, which enables Valen to exhibit strong human-interpretable characteristics when processing 3×3 progressive matrices. By examining the distribution of $\{P_{nm}\}$, we can inspect Valen’s interpretation of the progressive patterns in the current 3×3 matrix. The degree of human-interpretability provided by SBR to Valen can be quantified by assessing the accuracy of Valen’s interpretations of matrix progression patterns. The accuracy of SBR+Valen’s interpretations of progressive patterns on PGM is presented in Table II.

TABLE II
THE ACCURACY OF SBR+VALEN’S INTERPRETATIONS OF PROGRESSIVE PATTERNS ON PGM

Model	Accuracy(%)		
	shape	line	answer
SBR+Valen	99.7	99.9	99.4

C. progressive pattern generalization problem within PGM

The SBR method holds promise in addressing the progressive pattern generalization problem within PGM problem. In the context of progressive pattern generalization in PGM, the progressive patterns present in the training set do not directly appear in the test set. In other words, the metadata content within the training set is never encountered in the test set. This results in the supervisory signals utilized by our SBR method becoming out-of-distribution (OOD) supervisory signals at this juncture, which is a discouraging reality. However, we recognize that there are numerous methods available to tackle OOD problems, each with its own merits, but a common approach is model pretraining. We can leverage SBR to formulate a pretraining method to cope with the progressive pattern OOD problem. Specifically, we run SBR+Valen on the progressive pattern generalization problem as usual, subsequently reinitialize the parameters of the Progressive Pattern Extractor and Pattern Consistency Analyzer within the trained Valen, and finally utilize the partially parameter-initialized Valen to relearn the progressive pattern OOD problem.

The distribution of $\{P_{nm}|n \in [1, 9], m \in [1, M]\}_{v=1}^V$ planned by SBR on the progressive pattern generalization problems is biased and incomplete. However, the SBR method still provides guidance for Valen in decoupling M types of progressive patterns. The partially parameter-initialized approach adopted in this paper aims to enable Valen to discard the biased guidance introduced by SBR for the distribution of $\{P_{nm}\}_{v=1}^V$, while retaining the guidance provided by SBR for decoupling progressive patterns.

The relevant experimental results are recorded in Table III, The modules that require initialization are outlined with purple dashed lines within the Valen architecture presented in Figure 4.

TABLE III
GENERALIZATION RESULTS OF SBR IN PGM.

Dataset	Accuracy(%) SBR(pre-train)+Valen
Held-out Attribute shape-colour	12.8
Held-out Attribute line-type	21.4
Held-out Triples	28.1
Held-out Pairs of Triples	96.2
Held-out Attribute Pairs	96.9

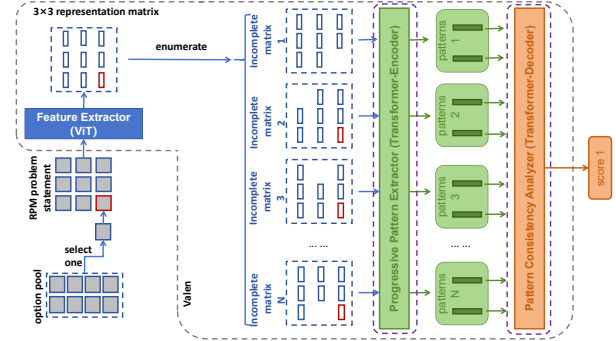


Fig. 4. Valen

D. supplementary content for the main text

This paper posits that planning the distribution of solutions to conform more closely to the distribution of correct solution is the key to enhancing the reasoning capabilities of solvers. Referring to the experiments recorded in Table III regarding PGM, it is notable that we did not conduct multi-combination experiments such as Funny+Valen+Tine. This decision was made due to the significant increase in Valen’s training duration when Funny and Tine are employed simultaneously. Additionally, given that the individual application of Funny, Tine, and SBR methods has already yielded impressive results for Valen, adequately demonstrating the paper’s hypothesis, we deemed it unnecessary to pursue combinations involving three or more methods, such as Funny+Valen+Tine.

Funny-Valen-Tine: Planning Solution Distribution Enhances Machine Abstract Reasoning Ability

Ruizhuo Song, Member, IEEE, Beiming Yuan

Abstract—The importance of visual abstract reasoning problems in the field of image processing is beyond words. Both Bongard-Logo problems and Raven’s Progressive Matrices (RPM) belong to the domain of visual abstract reasoning tasks, with Bongard-Logo categorized as image clustering reasoning and RPM involving image progression pattern reasoning. This paper introduces a novel baseline model, Valen, which falls under the umbrella of probabilistic highlighting models. Valen demonstrates remarkable performance in solving both RPM and Bongard-Logo problems, offering a versatile solution for these reasoning tasks. Our investigation extends beyond the application of Valen, delving into the underlying mechanisms of probability-highlighting solvers when tackling visual abstract reasoning problems. We revisit how these solvers handle instances in tasks like RPM and Bongard-Logo, realizing that they approximate the solution to each reasoning problem instance as a distribution delineated by primary and auxiliary samples. This led us to propose that the learning objective of probability-highlighting solvers is not the distribution of correct solutions but rather a distribution defined by both primary and auxiliary samples. To bridge the discrepancies, we introduced the Tine method, an adversarial learning-based approach designed to assist Valen in estimating a solution distribution closer to the correct one. However, Tine’s adversarial framework also introduces issues such as unstable training. Reflecting on Tine, we propose modeling the sample distribution of reasoning problems as a mixture of Gaussian distributions, leading to the development of the Funny method. Funny effectively models the sample distribution within reasoning problems as a mixture of Gaussian distributions, enabling Valen to more directly capture the true form of the correct solution distribution. Furthermore, we designed the SBR method to model the distribution of progressive patterns representation as a mixture of Gaussian distributions. Overall, this paper posits that the key to enhancing the ability of solvers to address visual abstract reasoning problems lies in explicitly planning the distribution of solutions to conform more closely to the distribution of correct solution.

Index Terms—Abstract reasoning, Raven’s Progressive Matrices, Bongard-Logo, Adversarial Learning, Gaussian Mixture Model.

I. INTRODUCTION

DEEP neural networks have made remarkable achievements in various fields, including computer vision [1]–

This work was supported by the National Natural Science Foundation of China under Grants 62273036. Corresponding author: Ruizhuo Song, ruizhuosong@ustb.edu.cn

Ruizhuo Song and Beiming Yuan are with the Beijing Engineering Research Center of Industrial Spectrum Imaging, School of Automation and Electrical Engineering, University of Science and Technology Beijing, Beijing 100083, China (Ruizhuo Song email: ruizhuosong@ustb.edu.cn and Beiming Yuan email: d202310354@xs.ustb.edu.cn).

Ruizhuo Song and Beiming Yuan contributed equally to this work.

[3], natural language processing [4]–[6], generative model [7]–[9], visual question answering [10], [11], and visual abstract reasoning [12]–[14].

Visual abstract reasoning plays a pivotal role in the field of image processing. It is not only one of the advanced tasks in image processing, requiring systems to recognize objects in images and understand the relationships between them for logical inference, but also a key driver for technological innovation and application expansion in image processing. By addressing visual abstract reasoning problems, new algorithms and techniques such as deep learning and graph convolutional networks can be explored and applied, thereby propelling extensive applications and developments in fields like autonomous driving, medical diagnosis, and security surveillance. However, this field still faces challenges such as insufficient and imbalanced data, as well as limited model interpretability. Future research will focus more on enhancing the robustness, real-time performance, and interpretability of algorithms to further elevate the potential and value of visual abstract reasoning technology.

The RPM problem [14] and the Bongard problem [12], [13] are two renowned examples within the realm of visual abstract reasoning. These two problems are the target problems that this paper aims to solve.

A. RAVEN and PGM

RPM [14], or Raven’s Progressive Matrices, is a classic visual reasoning intelligence test typically presented as a 3x3 matrix. It requires test-takers to observe and analyze visual features such as shape, size, direction, position, and their relationships within the problem statement, identify patterns or rules, and select an answer from given option pool that completes the matrix. Due to its non-verbal nature and value in assessing general intelligence, RPM is widely used in psychology, education, neuroscience, and other fields, serving as a tool for evaluating intelligence levels and studying human cognitive processes, intellectual development, and brain function. With the advancement of AI technology, researchers are exploring computer algorithms to solve RPM problems, albeit facing challenges. RAVEN [15] and PGM [16] are classic examples of RPM problems, with Figure 1 illustrating these two types of problems respectively.

B. Bongard-Logo

Distinct from the image progressive pattern reasoning problems like RPM, the Bongard problem [12], [13] belongs to the category of image clustering reasoning problems. It

arXiv:2407.02688v2 [cs.CV] 7 Jul 2024

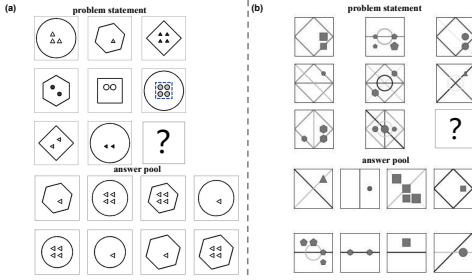


Fig. 1. RAVEN instance (a) and PGM instance (b)

typically involves multiple images divided into primary and auxiliary groups, with images in the primary group sharing an abstract concept governed by a specific rule and those in the auxiliary group deviating from these rules. Solving Bongard problems requires deep learning algorithms to accurately classify ungrouped images. As a specific instance within abstract reasoning, the Bongard-Logo problem [13] poses a significant challenge due to its inferential complexity. Each case comprises 14 images: six from the primary group, six from the auxiliary group, and two for classification. The grouping criterion relies on geometric shapes and their arrangement. Figure 2 illustrates a Bongard-Logo case.

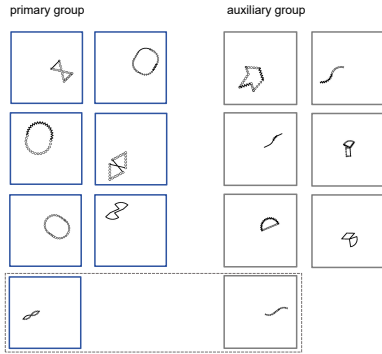


Fig. 2. Bongard-Logo instance

II. RELATED WORK

A. RPM solvers and Bongard-Logo solvers

There are numerous excellent solvers for RPM and Bongard-Logo problems, among which CoPINet [19], LEN+teacher [18], DCNet [20], NCD [22], SCL [23], SAVIR-T [24], PrAE [25], NVSA [27], ALANS [26], RS-TRAN [28] and CRAB [29] are notable RPM solvers, while SBPDL [30], PMoC [31] and Triple-CFN [32] are outstanding Bongard-Logo solvers. Since the method proposed in this paper is relatively independent and does not have a strong dependency on these existing works, the details about them will not be elaborated further.

III. METHODOLOGY

Both Bongard-Logo problems and Raven’s Progressive Matrices (RPM) fall under the umbrella of visual abstract reasoning tasks. Specifically, Bongard-Logo problems can be cate-

gorized as image clustering reasoning, while RPM challenges involve image progression pattern reasoning.

In this paper, we designed a general solver, Valen, for both RPM and Bongard-Logo problems. This paper proposes that to enhance the ability of solvers to address visual abstract reasoning problems, the distribution of solutions provided by the solver should be explicitly planned to better conform to the distribution of correct solutions. Therefore, we developed three accompanying methods: Funny, Tine, and SBR. These three methods all aim to explicitly plan the distribution of solutions generated by Valen.

Here we clarify a definition: in this paper, “primary samples” refer to those that align with the core patterns in reasoning problems, like correct RPM options or primary group samples in Bongard-Logo instances. Conversely, “auxiliary samples” are those that deviate from these patterns, such as incorrect RPM options or auxiliary group samples in Bongard-Logo problems.

IV. VALEN: A NEW BASELINE MODEL FOR RPM AND BONGARD-LOGO PROBLEMS

In this section, we introduce Valen (Visual Abstraction Learning Network), our baseline model designed to address both RPM, an image progressive pattern reasoning problem, and Bongard-Logo, an image clustering reasoning problem.

A. Valen targeting RPM problem

The RPM problem challenges participants to complete a 3×3 matrix of images by choosing answers from a pool of options. A correct answer is one that, when placed in the matrix, maintains a consistent and specific image progression pattern that can be deduced from the incomplete matrix, referred to as the problem statement [36].

This paper requires a baseline to support our reasoning work. This baseline is expected to determine the plausibility of an RPM matrix based on the progression patterns exhibited within it and assign a probability to reflect this plausibility.

In RPM problems, there exists a unique design where an incomplete RPM matrix (missing one image) can still convey a complete progression pattern. This design is essential as RPM serves as an assessment tool. Hence, this paper asserts that the reasoning process of a successful RPM problem solver should be schematically represented as illustrated in the Figure 3. As seen in the figure, our envisioned RPM

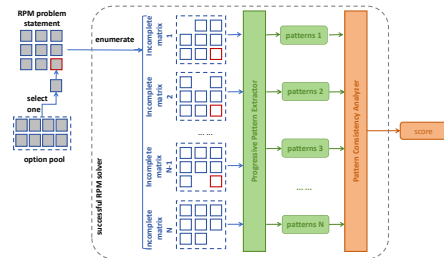


Fig. 3. The reasoning process of an envisioned RPM problem solver

solver consists of two modules: the Progressive Pattern Extractor and the Pattern Consistency Analyzer. Additionally,

our envisioned RPM solver can perform the following three reasoning processes: 1. The process indicated by the blue line: When the RPM problem statement is completed by an option from the option pool to form a full 3×3 progression matrix, the solver can enumerate all N types of incomplete matrix of this 3×3 matrix. 2. The process denoted by the green line: For each enumerated incomplete matrix, the Progressive Pattern Extractor extracts the progression pattern, resulting in a total of N sets of progression patterns. 3. The process marked by the orange line: The solver utilizes its Pattern Consistency Analyzer to evaluate the consistency of these N sets of progression patterns and outputs a score to quantify this consistency. This score also serves as the score for the corresponding option. The aforementioned three processes will also constitute the procedure of Valen.

Since this paper provides a clear definition of the reasoning process for a successful RPM solver, our designed Valen is derived by refining these three processes. Specifically, our Valen also consists of three processes: representation extraction of matrix and enumeration of incomplete matrix, extraction of progressive patterns from incomplete matrix, and consistency analysis of progressive patterns, which correspond to the aforementioned three processes respectively. We will introduce these three refined processes one by one.

1) *Representation extraction of matrix and enumeration of incomplete matrix*: In this paper, this process in Valen is designed as the structure shown in Figure 4. As shown in

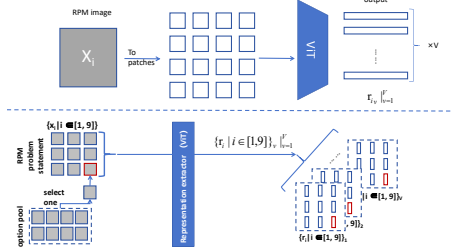


Fig. 4. Representation extraction of matrix

figure 4, when the problem statement of the RPM task is completed by a specific option to form a 3×3 progression matrix, denoted as $\{x_i | i \in [1, 9]\}$, Valen utilizes a basic Vision Transformer (ViT) as a feature extractor to obtain multi-viewpoint representations of $\{x_i | i \in [1, 9]\}$. These representations are denoted as $\{r_i | i \in [1, 9]\}_v$, where $v \in [1, V]$ and V represents the number of viewpoints, v represents the index of the viewpoint, and i represents the index of the image in the matrix. The subsequent processes in Valen will handle these multi-viewpoint representation matrices in parallel and equally. The method of processing RPM images into multi-viewpoint representations has been applied in previous works [24], [28].

Subsequently, these multi-viewpoint representations $\{r_i | i \in [1, 9]\}_v |_{v=1}^V$ will be enumerated by Valen to generate all possible incomplete representations matrix. The enumeration results are illustrated in the Figure 5. We denote these enumerated multi-viewpoint incomplete representation matrices as $\{r_{ni} | n \in [1, 9], i \in [1, 9], i \neq n\}_v |_{v=1}^V$, where n represents

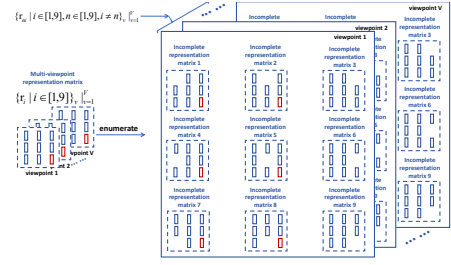


Fig. 5. Enumeration results of incomplete matrix

the index of the incomplete representation matrix, and i still represents the index of the representation within the incomplete matrix. Notably, the last item of the enumeration is the matrix with a incomplete option position, denoted as $\{r_{9i} | n \in [1, 9], i \in [1, 8]\}_v |_{v=1}^V$.

2) *Extraction of progressive patterns from incomplete matrix*: In Valen, this process is undertaken by a Transformer-Encoder. Specifically, we use a standard Transformer-Encoder to process all the previously enumerated multi-viewpoint incomplete representation matrices, with the processing procedure illustrated in Figure 6. The figure illustrates the process

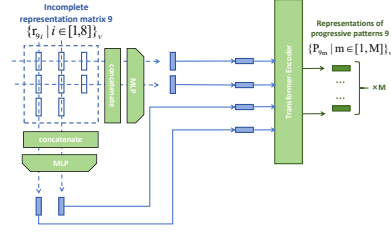


Fig. 6. Extraction of progressive patterns from incomplete matrix

of the Transformer-Encoder handling $\{r_{9i} | i \in [1, 8]\}_v$, which represents the last item of the enumeration results of incomplete representation matrices from a specific viewpoint v . The process of handling other incomplete representation matrices $\{r_{ni} | n \in [1, 8], i \in [1, 9], i \neq n\}_v$ is similar to the one shown in the figure, with no essential differences.

In the figure 6, we can observe that we use an MLP to extract all row and column progressive information from the incomplete representation matrix $\{r_{9i} | i \in [1, 8]\}_v$. Subsequently, we process all four row and column progressive information using a standard Transformer-Encoder to obtain M representations of progressive patterns. M is a hyperparameter that can be freely set, and in this paper, it is set to 2. The impact of setting M to other values on Valen is not explored in this paper. This asymmetric seq-to-seq implementation (four-to- M) has been introduced in related techniques of ViT [17]. After processing all the incomplete representation matrices $\{r_{ni} | n \in [1, 9], i \in [1, 9], i \neq n\}_v |_{v=1}^V$ using the standard Transformer-Encoder, we obtain all multi-viewpoint progressive pattern representations $\{P_{nm} | n \in [1, 9], m \in [1, M]\}_v |_{v=1}^V$.

3) *Consistency analysis of progressive patterns*: In this process, Valen will evaluate the consistency among these multi-viewpoint progressive pattern representations $\{P_{nm} | n \in$

$[1, 9], m \in [1, M]\}_v|_{v=1}^V$. The task of this consistency analysis will be accomplished by the Transformer-Decoder. The process of evaluating the consistency of the progressive pattern representations $\{P_{nm}|n \in [1, 9], m \in [1, M]\}_v$ from a specific viewpoint v can be conducted using a Transformer-Decoder, as illustrated in Figure 7.

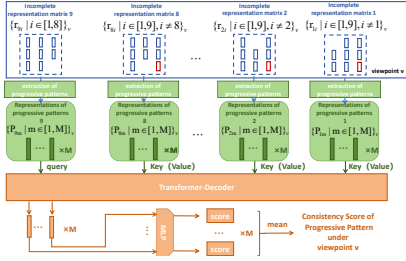


Fig. 7. Evaluating the consistency of the progressive patterns representation $\{P_{nm}|n \in [1, 9], m \in [1, M]\}_v$

In the figure 7, we can observe that the progressive pattern representations $\{P_{9m}|m \in [1, M]\}_v$ extracted from the incomplete representation matrix $\{r_{9i}|i \in [1, 8]\}_v$ are used as queries, while the other progressive pattern representations $\{P_{nm}|n \in [1, 8], m \in [1, M]\}_v$, which are extracted from the incomplete representation matrices $\{r_{ni}|n \in [1, 8], i \in [1, 9], i \neq n\}_v$, serve as key-value pairs input into the Transformer-Decoder to compute the output vector set. The M vectors within the output vector set are then individually mapped to a score by a new MLP. These mapped M scores are summed to obtain the consistency score of the progressive patterns under viewpoint v .

Subsequently, We calculate the average of the progressive pattern consistency scores obtained from all viewpoints to determine the overall viewpoint score for the corresponding option. Finally, we employ cross-entropy as the loss function to constrain the scores of all options according to the logic of the RPM task, in order to optimize the learnable parameters involved in the aforementioned three processes.

B. Valen targeting Bongard-Logo problem

We consider Valen as a good baseline model for dealing with image progressive pattern reasoning problems, but it can also handle image clustering reasoning problems such as Bongard-Logo. To adapt Valen to the Bongard-Logo problem, we need to transform this problem accordingly.

In a particular instance of the Bongard-Logo problem, we use x_i to represent all the images. Specifically, the images in the primary group of this instance are denoted by $\{x_i|i \in [1, 6]\}$, while those in the auxiliary group are represented by $\{x_i|i \in [8, 13]\}$. Furthermore, x_7 represents the test sample that should be assigned to the primary group, and x_{14} represents the test sample that should be assigned to the auxiliary group.

This paper proposes that we can adopt different perspectives to view image clustering reasoning problems, such as the Bongard-Logo problem. Specifically, we can treat them as an option evaluation problem akin to the RPM problem. To elaborate, the images in the primary group $\{x_i|i \in [1, 6]\}$

can be regarded as a problem statement similar to that in the RPM problem, while the test images and images in the auxiliary group $\{x_i|i \in [7, 14]\}$ can be seen as an option pool analogous to the one in the RPM problem. This transformation process can be visualized through Figure 8. After

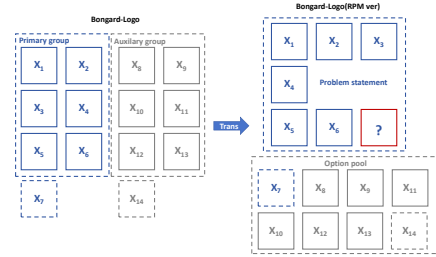


Fig. 8. Transformation of Bongard-Logo problem

such transformation, Valen can be effectively applied to image clustering reasoning problems like the Bongard-Logo problem.

It is noteworthy that when migrating Valen to Bongard-Logo, some adjustments are still necessary to accommodate the data characteristics of Bongard-Logo. Specifically, due to the scarcity of training instances in the Bongard-Logo problem, the ViT-based image representation extractor may struggle to perform effectively [17], [28]. Furthermore, although we transform the Bongard-Logo problem into an RPM-like format, it is unnecessary to analyze the progressive patterns among Bongard-Logo images, as such patterns do not exist in clustering reasoning problems like Bongard-Logo.

Therefore, we have redesigned the image representation extractor, originally illustrated in Figure 4, into a convolutional network concatenated with a Transformer-Encoder. The new extractor design can be visualized in Figure 9. In the

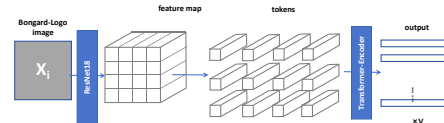


Fig. 9. Representation extraction of Bongard-Logo image

figure 9, we can observe that when a Bongard-Logo image is processed by the new Valen’s feature extractor, it is first encoded into a feature map by ResNet18. Subsequently, this feature map is decomposed into multiple tokens and fed into a standard Transformer-Encoder to obtain multi-viewpoint representations. Such a design allows for the combination of CNN’s ability to analyze a smaller number of samples [1]–[3], [17] and ViT’s ability to analyze samples from multiple viewpoint [24], [28]. This design has been applied in previous work [24].

Additionally, we have simplified the incomplete matrix progressive pattern extractor, which was originally intended to be structured as shown in Figure 6, into the form illustrated in Figure 10. In the figure10, we can see that we have abandoned the use of MLP to extract the row and column progressive information from the incomplete matrix in Bongard-Logo, because the transformed Bongard-Logo problem only contains

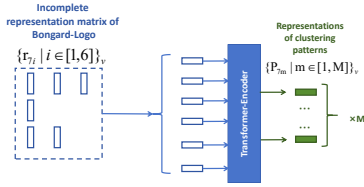


Fig. 10. Pattern extraction of Bongard-Logo incomplete matrix

clustering patterns and not progressive patterns. Instead, we directly feed the representations of all images within the incomplete matrix of Bongard-Logo as tokens into the Transformer-Encoder to extract M clustering patterns of Bongard-Logo. When Valen processes Bongard-Logo problems, M is set to 6.

V. TINE, A METHOD FOR ADVANCING THE SOLUTION DISTRIBUTION BOUNDARY

Current visual abstract reasoning problem solvers, including Valen, mostly follow a pattern: solvers are keen on assigning probabilities to each option of reasoning problems. The loss functions designed for these solvers are diverse, and the backbone network designs of these solvers vary greatly, but most of them adhere to this paradigm. We name this type of solver as “probability-highlighting solver”.

Therefore, we can interpret these solvers as a conditional probability distributions obeyed by abstract reasoning problems, or understand them as providing distributions of solutions to abstract reasoning problems. If we use RPM solvers as examples, then these solvers can be abstracted as a conditional probability distribution, denoted as $P(x_\alpha | \{x_i\}_{i=1}^8; \theta)$. (Accordingly, when Valen is applied to Bongard-Logo problems, it can be abstracted as a conditional probability distribution $P(x_\alpha | \{x_i\}_{i=1}^6; \theta)$). In this context, the two conditions of the conditional probability distribution $P(x_\alpha | \{x_i\}_{i=1}^8; \theta)$ are the statement of the reasoning problem $\{x_i\}_{i=1}^8$ and the optimizable parameters θ of the solver. Here, the x_α refers to the option that is pending verification. This conditional distribution implies that, when given a problem statement $\{x_i\}_{i=1}^8$ and an option x_α , it is possible to calculate the probability of x_α being a solution to $\{x_i\}_{i=1}^8$.

The optimization of probability-highlighting solver can be regarded as optimizing the conditional probability distribution $P(x_\alpha | \{x_i\}_{i=1}^8; \theta)$. A wide range of loss functions can be used for optimization, but they all share the same objective: to assign high probabilities to the primary samples in the probability distribution $P(x_\alpha | \{x_i\}_{i=1}^8; \theta)$ and low probabilities to the auxiliary options. Such an optimization objective makes us realize that the optimization process of the probability-highlighting solver is not aimed at fitting the distribution of correct solutions to visual abstract reasoning problems, but rather is dedicated to fitting a distribution jointly delimited by primary and auxiliary samples.

To simplify the explanation of our findings, we assume that the conditional probability distribution $P(x_\alpha | \{x_i\}_{i=1}^8; \theta)$ follows a Gaussian distribution. Consequently, we can explicitly identify the distribution $P(x_\alpha | \{x_i\}_{i=1}^8; \theta)$ as the distribution

$P(x_\alpha | \{x_i\}_{i=1}^8; \mu_\theta, \sigma_\theta)$. Then, the negative logarithm of the probability density function of $P(x_\alpha | \{x_i\}_{i=1}^8; \mu_\theta, \sigma_\theta)$ can be expressed as follows:

$$-\log(P(x_\alpha | \{x_i\}_{i=1}^8; \mu_\theta, \sigma_\theta)) = \frac{(x_\alpha - \mu_\theta)^2}{2\sigma_\theta^2} - \log(|\sigma_\theta|) \quad (1)$$

Evidently, we have omitted the constant term $-1/2 \log(2\pi)$. In this formula, μ_θ and σ_θ respectively represent the mean and standard deviation of $P(x_\alpha | \{x_i\}_{i=1}^8; \theta)$. Since we have defined the form of distribution $P(x_\alpha | \{x_i\}_{i=1}^8; \theta)$ as a Gaussian distribution, we consequently abstract the optimizable parameters θ into optimizable mean μ_θ and standard deviation σ_θ .

Optimizing the distribution $P(x_\alpha | \{x_i\}_{i=1}^8; \mu_\theta, \sigma_\theta)$ using the loss function is equivalent to optimizing the values of μ_θ and σ_θ . Our optimization objective is that when primary samples (the correct options in an RPM problem, or the samples within the main group in a Bongard-Logo problem) are plugged into formula (1), we expect to obtain a smaller value. Conversely, when auxiliary samples (the incorrect options in an RPM problem, or the samples within the auxiliary group in a Bongard-Logo problem) are plugged into formula (1), we hope that the formula returns a larger value.

Evidently, constraining the return value of the formula to achieve a minimum is equivalent to optimizing the value of μ_θ in the formula. Conversely, constraining the return value to achieve a maximum is equivalent to minimizing the value of σ_θ in the formula. In other words, the probability-highlighting solver positions the mean of the solution distribution $P(x_\alpha | \{x_i\}_{i=1}^8; \theta)$ for the reasoning problem through primary samples, while the standard deviation of the solution distribution is constrained by auxiliary samples.

It appears to be a discouraging reality that the learning objective of a probability-highlighting solver is not to determine the distribution of the correct solutions to reasoning problems, but rather to approximate a distribution that is delimited by both primary and auxiliary samples within those problems. This suggests that the reasoning accuracy of the probability-highlighting solver is constrained. The standard deviation of the distribution delimited by the auxiliary samples is necessarily greater than or equal to the standard deviation of the correct solution distribution. In other words, the distribution delimited by both primary and auxiliary samples is often much coarser than the distribution of correct solutions. Aiming to approximate the former as the optimization objective is akin to “aiming for mediocrity and achieving even less”. This discouraging reality can be visualized in Figure 11. Note that the figure 11 is intended to schematically represent our analysis results, rather than to depict the actual form of the solution distribution or the correct solution distribution.

This paper argues that to further improve the reasoning accuracy of Valen in solving RPM problems and Bongard-Logo problems, it is necessary to provide Valen with more judicious auxiliary samples. By “more judicious auxiliary samples,” we refer to those that can better delimit the solution distribution provided by Valen. These more judicious auxiliary samples have the potential to narrow down the standard deviation of the

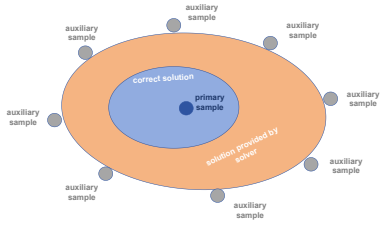


Fig. 11. Schematic diagram of the relative relationship between the solution distribution, the correct solution distribution, and the primary and auxiliary samples.

solution distribution. The visualization of these more judicious auxiliary samples can be found in Figure 12.

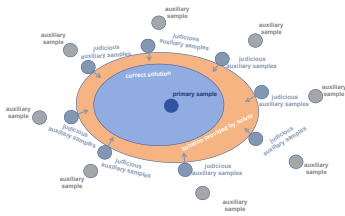


Fig. 12. judicious auxiliary samples

As seen in the figure 12, the judicious auxiliary samples we desire are those that appear more authentic or closer to the primary samples from Valen’s perspective, compared to the original auxiliary samples provided in the reasoning problems. Since the property of being “judicious” is evaluated from Valen’s perspective, whether an auxiliary sample is judicious or not, and the extent of its judiciousness, lacks interpretability from a human perspective. This implies that, relative to the primary samples, samples with smaller attribute shifts or fewer shifted attributes may not necessarily be considered more judicious from Valen’s perspective.

Therefore, this paper argues that we can adopt an adversarial learning strategy to provide Valen with auxiliary samples that are more judicious from Valen’s perspective. Given this insight, we design Tine (Technique for edge Identification of solution distribution based on adversarial Networks) method. Specifically, we intend to emulate adversarial generation techniques similar to GAN [7] or WGAN [33] to generate more judicious samples for Valen. However, unlike GAN or WGAN, whose objective is to train robust and high-performance generators, our utilization of adversarial learning aims to refine Valen, which serves as the discriminator in this context.

Our objective is to design an auxiliary sample generator for Valen. The task of this generator is clear: to produce auxiliary samples that can achieve higher scores (probability) in Valen compared to the original auxiliary samples provided in the reasoning tasks. Conversely, Valen’s role is to classify these auxiliary samples as low-scoring ones. During the training process, the parameters of Valen and this generator are updated alternately and exclusively, with their performance gradually refined through adversarial learning, which is a common process in adversarial learning.

Given that our pursuit is to generate more judicious auxiliary samples from Valen’s perspective, we are not concerned with their interpretability, attribute geometry, or whether they strictly conform to the nature of reasoning problems. Therefore, we believe that instead of forcing the generator to produce image-based auxiliary samples, which would incur greater computational overhead and optimization difficulties, it is more effective to generate representations of judicious auxiliary samples. By solely generating multi-viewpoint representations of reasoning problems, the generator’s structure becomes simpler and easier to optimize. Consequently, our generator is designed as shown in Figure 13. The figure 13 depicts Valen, which is tailored for addressing the RPM problem, and its accompanying auxiliary sample representation generator. Since we have already transformed the Bongard-Logo problem into an RPM-like problem, we will not further elaborate on the structure of the generator for the Bongard-Logo version.

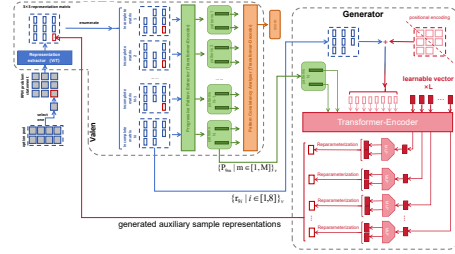


Fig. 13. The structure of the generator associated with Valen

As depicted in Figure 13, the left gray dashed box encloses the previously designed Valen, while the right gray dashed box encloses the generator designed for Valen. The figure 13 shows that the backbone of this generator is a standard Transformer-Encoder, which generates representations of more judicious auxiliary samples based on the representations of the abstract reasoning problem statement $\{r_i | i \in [1, 8]\}_v$, the progressive patterns $\{P_{9m} | m \in [1, M]\}_v$ of the statement, and L learnable vectors. Both the representations of the statement and their progressive patterns are provided by Valen, while the L learnable vectors require additional establishment for the generator. It is noteworthy that when dealing with PGM problems in RPM tasks, we have designed special positional encoding for the representations of the problem statement. This positional encoding can be specifically attached to incomplete matrices with missing option positions and is set symmetrically along the diagonal. After the Transformer-Encoder processes the input representations (i.e., $\{r_i | i \in [1, 8]\}_v$, $\{P_{9m} | m \in [1, M]\}_v$ and L learnable vectors) and generates the output, we extract and save those L optimizable vectors from the output. These L (processed) output learnable vectors are then individually processed by an MLP into vectors of double length. These L doubled-length vectors are transformed into L vector using the reparameterization technique [8]. The process of reparameterization, which is a practical approach used in VAE [8], can be visualized as Figure 14. These L reparameterized vector are regarded as the representations of L auxiliary samples. It is worth noting that L is a hyperparam-

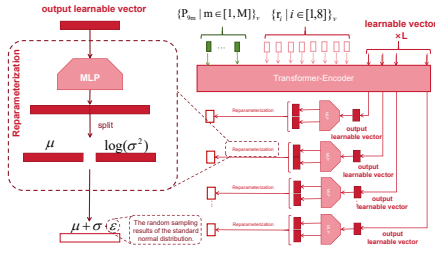


Fig. 14. Reparameterization

eter that can be freely set, determining how many judicious auxiliary samples Tine generates for Valen in one instance. In this paper, L is set to 9.

In summary, our Tine method is proposed after summarizing the working principles of probability-highlighting solvers such as Valen. We believe that such solvers establish a solution distribution for each instance of a reasoning problem, with the optimization objective being to assign high probability to primary samples and low probability to auxiliary samples. This means that the optimization target of the solution distribution is not aligned with the distribution of correct solutions to the reasoning problems, but rather with the distribution delimited by both primary and auxiliary samples. Unfortunately, this delimited distribution is often much coarser than the correct solution distribution. To make the distribution delimited by both primary and auxiliary samples closer to the correct solution distribution, we designed Tine based on adversarial learning. Although subsequent experiments demonstrated that Tine can effectively improve Valen’s performance, we believe that the Tine method still fails to address the underlying essence of the problem. Therefore, further exploration is conducted in this paper.

VI. FUNNY: METHOD FOR PLANNING THE DISTRIBUTION OF REASONING PROBLEM SAMPLES.

Based on the analysis in the previous section, auxiliary samples provided in reasoning tasks constrain the standard deviation of the solution distribution $P(x_\alpha | \{x_i\}_{i=1}^8; \theta)$, while primary samples locate the mean of the solution distribution $P(x_\alpha | \{x_i\}_{i=1}^8; \theta)$. The Tine method generates more judicious auxiliary samples to further constrain the standard deviation. Although experimental results demonstrate the effectiveness of Tine, it remains uncertain whether Tine constrains the standard deviation too little or not enough. Furthermore, Tine based on adversarial learning also encounters all the issues associated with adversarial learning, such as unstable training processes and difficulties in determining the completeness of training. Given this series of challenges, this paper proposes the Funny (Framework Utilizing Neural Networks for Yielding Image Representation Distribution) method.

Our Funny method argues that instead of laboriously adopting adversarial learning strategies to make the solution distribution $P(x_\alpha | \{x_i\}_{i=1}^8; \theta)$ provided by the solver closer to the correct solution distribution, it is more effective to directly specify the range of correct solutions or, alternatively, to explicitly define the details of the correct solution distribution.

This paper will next analyze the definition of correct solutions for image progressive pattern reasoning problems such as RPM and image clustering reasoning problems such as Bongard-Logo.

According to the design of RPM problems, the attributes of an image within the RPM problem are divided into key attributes related to reasoning and non-key attributes unrelated to reasoning. The design purpose of attributes unrelated to reasoning is to interfere with the solver’s reasoning and test its ability to filter attributes. This paper has discovered a point that cannot be neglected: attributes are the only factor that determines the specificity of RPM images. Any two RPM images with the same key attributes have the same identity in the reasoning process, regardless of how different their non-key attributes are. This implies that any sample whose key attributes pass the verification can be considered a correct solution to the RPM problem. For instance, in the RAVEN problem [15], the angle of an entity is considered a non-key attribute that is unrelated to reasoning, while attributes such as color, size, shape, and position are all key attributes. This leads to the situation where a white, medium-sized hexagon positioned in the center retains its reasoning identity regardless of how it is rotated. No matter how it rotates, it will not be transformed from a correct solution to an incorrect one or vice versa.

The design of correct solutions for Bongard-Logo problems is much more complex. The reasoning identity of a Bongard-Logo sample is determined by the context within the specific instance it belongs to. Among the various attributes of a sample, which are key attributes and which are non-key attributes are influenced by the context within the relevant instance. In Bongard-Logo problems, some instances focus on more macroscopic attributes of the image, such as its closure and concavity & convexity; while other instances focus on more detailed attributes, such as the number of entities in the image and the order of their arrangement. This is different from RPM problems, where the key and non-key attributes are consistent across all instances within the RPM.

Given the differences in determining correct solutions, or in identifying key and non-key attributes, between Bongard-Logo and RPM problems, the application of our proposed Funny approach differs when applied to these two types of problems. We will discuss them separately.

A. Funny for RPM problems

Given that the key attributes and non-key attributes in the RPM problem are fixed, with key attributes being key across all instances and non-key attributes being unfavored in any instance, this paper proposes that the representations of samples with the same key attributes can be mapped into a single Gaussian distribution. Within this Gaussian distribution, the key attributes of the samples are identical, but the non-key attributes vary. Consequently, the distribution of representations for all samples in the entire RPM problem is formulated as a mixture of Gaussian distributions. By exposing Valen to this mixture of Gaussian distributions instead of individual sample representations, we effectively clarify the distribution

of correct solutions for Valen. Our intention is to achieve the transformation of the sample representation space as illustrated in the Figure 15. Therefore, the purpose of the Funny method

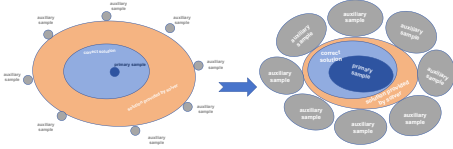


Fig. 15. Modeling the representation distribution as a mixture of Gaussian distributions.

is to plan the distribution of samples in the RPM problem as a mixture of Gaussian distributions, with the key attributes serving as the component means.

The design of Valen’s Funny method, applied to tackle the RPM problem, is quite straightforward. The Funny method separately extracts the key attributes and non-key attributes of RPM images, treating the key attributes as the center and the non-key attributes as biases relative to this center. Therefore, we refer to the representation of the key attributes extracted from the RPM image x_i as $center_i$, and the representation of the non-key attributes as $bias_i$. Interestingly, the sum of $center_i$ and $bias_i$ can be viewed as samples drawn from a Gaussian distribution $N(center_i, \sigma^2)$, which represents a distribution with a mean of $center_i$ and an unknown variance σ^2 . When the $bias_i$ follow a standard normal distribution, this Gaussian distribution can be considered as $N(center_i, 1)$, which is a distribution with a mean of $center_i$ and a variance of 1. In this scenario, representations of samples with the same key attributes but different non-key attributes only differ in their biases. This implies that the Funny method successfully maps representations of samples with the same key attributes into the same Gaussian distribution.

Based on this hypothesis, we design a multi-viewpoint image representation extractor as illustrated in Figure 16, which replaces Valen’s original representation extractor when equipped with the Funny method. As can be seen in the figure

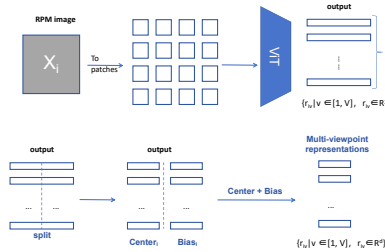


Fig. 16. Funny representation extractor

16, Funny encodes the image sample x_i of the reasoning problem into two sets of homomorphic multi-viewpoint representations, named $center_i$ and $bias_i$ respectively. The final multi-viewpoint representation r_i of the image x_i extracted by the Funny representation extractor is obtained by summing $center_i$ and $bias_i$.

However, the new representation extractor of the Funny method, which encodes images x_i into $center_i$ and $bias_i$, still

faces two challenges: 1. How to ensure that the $center_i$ stores key attributes while the $bias_i$ stores non-key attributes? 2. Given that the union of key and non-key attributes constitutes all attributes, how to guarantee that the combination of $center_i$ and $bias_i$ can store all attributes of the image x_i ? These two questions pose challenges to both the center and bias individually and collectively.

This paper argues that by enforcing $bias_i$ to follow a standard normal distribution $N(0, 1)$ and simultaneously enforcing all random sampling results from a Gaussian distribution $N(center_i, 1)$ to assume the same reasoning identity, it can be ensured that $center_i$ stores at least the key attributes. This is because, when samples drawn from Gaussian distribution $N(center_i, 1)$ all share the same reasoning identity, $bias_i$, which follows a standard normal distribution $N(0, 1)$, ceases to influence the reasoning, and $center_i$ takes full responsibility for the reasoning task, indicating that $center_i$ stores at least the key attributes at this point.

Furthermore, to ensure that the combination of $center_i$ and $bias_i$ can store all attributes within image x_i , and consequently guarantee that the $bias_i$ stores the image attributes omitted by the $center_i$, it suffices to maximize the mutual information between combination of $center_i$ and $bias_i$ and all attributes within image x_i . The most direct method to maximize the mutual information between image attributes and image representations is to append an additional reconstruction task. Therefore, when the Valen framework incorporates the Funny method, its structure should be as illustrated in the Figure 17.

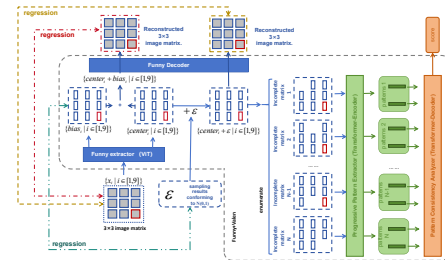


Fig. 17. The Valen framework incorporates the Funny method

In the figure 17, we can observe that the representation of key attribute, which is $\{center_i | i \in [1, 9]\}$, extracted by the Funny extractor for a 3×3 image matrix $\{x_i | i \in [1, 9]\}$ is superimposed with the sampling results ϵ from a Gaussian normal distribution $N(0, 1)$ and then fed into the regular Valen framework to undertake subsequent reasoning tasks. This is done to clarify with the help of Valen that the representations drawn from the Gaussian distribution $N(center, 1)$ have the same reasoning identity.

Furthermore, in the figure 17, we can observe that Funny introduces three additional regression tasks based on mean squared error (MSE) loss to Valen, which are indicated by dashed lines in red, yellow, and green. The green dashed line indicates the regression task between the representation of non-key attributes, which is $\{bias_i | i \in [1, 9]\}$, and the random sampling results ϵ from the standard normal distribution $N(0, 1)$. It is worth noting that the ϵ here needs to

be resampled and cannot be the one previously superimposed on the $\{center_i | i \in [1, 9]\}$. The objective of this green task is to enforce the bias to conform to the standard normal distribution $N(0, 1)$. The red and yellow dashed lines indicate the two regression tasks performed by the Funny decoder. The task indicated by the red dashed line aims to reconstruct the corresponding RPM image x_i from the representation obtained by adding $center_i$ and $bias_i$. The task indicated by the yellow dashed line aims to reconstruct RPM images from the representation obtained by adding $center_i$ and ϵ .

The objectives of these two reconstruction tasks are vastly different. The reconstruction task indicated by the red dashed line is aimed at maximizing the conditional distribution $P(x_i | center_i + bias_i)$ during the training process of the Funny decoder. On the other hand, the reconstruction task indicated by the yellow dashed line is intended to ensure that the output of the Funny decoder follows the distribution of RPM images, thereby guaranteeing that the Funny decoder can effectively function as a distribution transformation function.

The objective of the red reconstruction task, which is to maximize the conditional distribution $P(x_i | center_i + bias_i)$, is equivalent to maximizing the mutual information between the attributes of x_i and $center_i + bias_i$. This mutual information can be calculated using the following formula:

$$MI(x_i, center_i + bias_i) = H(x_i) - H(x_i | center_i + bias_i) \quad (2)$$

where $H(x_i)$ is the entropy of x_i , and $H(x_i | center_i + bias_i)$ is the conditional entropy of x_i given $center_i + bias_i$. This formula quantifies the amount of information shared between x_i and the combination of $center_i$ and $bias_i$. Additionally, the operations similar to the yellow reconstruction task, which involve constraining the output of the decoder to follow a certain distribution through MSE-based reconstruction tasks, have already been well-established and widely used in VAE [8].

Our design intention for Funny is quite clear. We hope that, with the assistance of Valen, Funny can compel $center_i$ to store more key attributes related to reasoning, while $bias_i$ accumulates more non-key attributes unrelated to reasoning that could potentially interfere with it. By doing so, we aim to model the distribution of multi-viewpoint representations, generated by the $center_i + bias_i$, as a mixed Gaussian distribution that aids Valen in its reasoning process. The relationship between Funny and Valen is mutually beneficial and symbiotic. Although subsequent experiments demonstrated that Funny is a significantly effective method, given the fact that obtaining disentangled representations under unsupervised learning is not achievable [40], this paper holds a pessimistic attitude towards the extent of Funny’s decoupling of key and non-key attributes.

B. Funny not funny

What is of paramount importance is that, a Funny decoder with a conventional structure cannot bear the aforementioned theoretical framework. If we apply a deconvolution structure to the backbone of the Funny decoder, its optimization becomes

extremely challenging, making it difficult to achieve satisfactory regression results and supervise the mutual information between $center_i + bias_i$ and x_i . Alternatively, if we replace the Funny decoder with a ViT structure symmetric to the representation extractor, although we obtain excellent regression results, it leads to a decrease in the normal reasoning accuracy of Valen instead of an increase.

Unfortunately and unfunny, there is a gap between theory and practice. This paper speculates that this may be due to the impact of the regression task in Funny on the parameter optimization of the reasoning task in Valen. If we choose the normal ViT as the Funny decoder, the introduced regression task will be completed before the Valen’s reasoning task, because the optimization speed of the regression task is faster than that of the reasoning task at this time. We posit that the premature completion of the regression task may result in the $center_i$ storing more non-key attribute. Because we have set up the regression task from $center_i + \epsilon$ to x_i . This paper speculates that this might be the issue: when the regression task approaches completion prematurely, it may lead to $center_i$ falling into the gradient vanishing zone, subsequently rendering it difficult for $center_i$ to make further optimizations for the reasoning task. The non-key attribute stored in $center_i$ can disrupt the reasoning process of Valen. An attempt was made to linearly search for the scaling coefficient between the MSE-based regression task introduced by Funny and the CE-based reasoning task in Valen, but it did not yield an effective solution. Anyway, this paper does not intend to bridge this gap between theory and practice by adjusting the scaling coefficients among the various terms in the loss function.

Fortunately and funny, this paper presents a novel decoder architecture, which we term the “Half-split Decoder” to address this issue. The structure of our designed Half-split Decoder is illustrated in the Figure 18. The upper half,

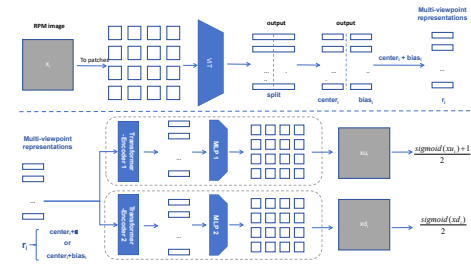


Fig. 18. Half-split Decoder

separated by the blue dashed line in figure 18, represents the representation extractor of Funny, which has been previously shown in Figure 16. The lower half depicts the structure of our designed Half-split Decoder.

In the figure 18, we can observe that our Half-split Decoder is composed of two identical structures, with each structure’s parameters optimized independently without parameter sharing. It is evident that each individual structure resembles an inverted version of a ViT [17], which we will not delve into further in this paper. These two identical structures regress the multi-viewpoint representation r_i into two outcomes, xu_i and xd_i , respectively. Here r_i can be derived either by summing

$center_i$ with ϵ or by summing $center_i$ and $bias_i$, corresponding to the two regression requirements of Funny. However, the core of the Half-split Decoder lies not in these structures but in the two distinct activation functions illustrated in the figure 18. We represent these two activation functions as follows:

$$f_1(xu_i) = \frac{\text{Sigmoid}(xu_i) + 1}{2}, f_2(xd_i) = \frac{\text{Sigmoid}(xd_i)}{2} \quad (3)$$

In the above equation, it is evident that the value range of $f_1(xu_i)$ lies within $(0.5, 1)$, while the value range of $f_2(xd_i)$ belongs to $(0, 0.5)$. Although the value ranges of both $f_1(xu_i)$ and $f_2(xd_i)$ differ from the value range of the original RPM image x_i , which is $(0, 1)$, we still compute the MSE loss between $f_1(xu_i)$ and x_i , as well as between $f_2(xd_i)$ and x_i . The sum of these two errors is used as the new loss function for the two regression tasks associated with the Funny decoder. This loss function can be represented by the following equation:

$$\ell_{\text{Funny}} = \text{MSE}(f_1(xu_i), x_i) + \text{MSE}(f_2(xd_i), x_i) \quad (4)$$

When both xu_i and xd_i in the formula are decoded from $center_i + bias_i$, the loss function is used to supervise the Mutual Information $\text{MI}(x_i, center_i + bias_i)$. Conversely, when both xu_i and xd_i are decoded from $center_i + \epsilon$, the loss function is employed to supervise the distribution that the output of the Funny decoder follows.

This Half-split Decoder can ensure that the loss of the regression task introduced by Funny does not decrease to zero in the early stage of the reasoning task of Valen, thereby preventing the multi-view representation from becoming stagnant.

C. Funny for Bongard-Logo problem

Funny is inherently a method that analyzes the key degree of sample attributes and modifies the sample representation space accordingly. Since the key degree of an attribute in Bongard-Logo is determined by contextual information, the previous form of Funny is difficult to directly transfer to the Bongard-Logo problem. Therefore, we innovate the Funny method.

This paper argues that we can seek a series of unlearnable Bongard-Logo image sample mapping functions $F(x_i)$ that do not alter the key degree of image attributes in the current contextual environment. Additionally, these functions do not change the key attributes of the input image but produce varying degrees of alteration to non-key attributes. Clearly, we have not abandoned the motivation of Funny: to make it explicit to Valen that key attributes determine reasoning identity, while non-key attributes do not affect reasoning identity. The previous form of Funny achieved this by mapping the representations of samples with the same key attributes into a Gaussian distribution with a variance of 1.

So, how do we find such functions? Through Human-in-the-Loop (HITL). HITL refers to situations where human experts or users intervene and provide feedback or guidance during the operation or training of machine learning or deep learning models. By analyzing the three coexisting concepts in Bongard-Logo, we subsequently discovered that some direct data augmentation methods, such as horizontal or vertical flipping, and 90-degree, 180-degree, and 270-degree rotations,

can effectively serve as the function $F(x_i)$. Therefore, when we intend to apply the Funny method to Valen for addressing the Bongard-Logo problem, it suffices to randomly apply the aforementioned data augmentation methods to the training samples x_i during the regular training process of Valen. It is noteworthy that, unlike in the Bongard-Logo problem, these data augmentation methods may disrupt the key attributes in RPM problem. In other words, the Funny method tailored for the Bongard-Logo problem cannot be transferred to RPM problems, and vice versa.

VII. SBR: METHOD FOR PLANNING THE DISTRIBUTION OF REASONING PATTERNS.

This paper suggests that we should also plan the distribution of the pattern representation $\{P_{nm}|m \in [1, M]\}_v$ extracted by Valen for visual abstract reasoning problems, so that it is closer to the distribution of the correct solution's pattern.

However, there are no key or non-key parts in the pattern representation $\{P_{nm}|m \in [1, M]\}_v$ encoded by Valen for RPM problems or Bongard-Logo problems, and even currently, the pattern representation $\{P_{nm}|m \in [1, M]\}_v$ lacks any interpretability. Therefore, our Funny method is difficult to directly apply to the pattern representations $\{P_{nm}|m \in [1, M]\}_v$.

Therefore, we have designed a new method, SBR (Supervised Representation Distribution Planning Method). This method can explicitly model the distribution of $\{P_{nm}|m \in [1, M]\}_v$ as a mixture of Gaussian distributions. The idea of SBR is straightforward: SBR defines the distribution form of $\{P_{nm}|m \in [1, M]\}_v$ as a mixture of Gaussian distributions and provides additional supervisory signals for the mean and variance of each sub-component in this hypothetical distribution.

When establishing a Gaussian Mixture Model (GMM), providing means, covariance matrices, and component weights is a necessary procedure. However, the objective of this paper is to model the distribution of pattern representations $\{P_{nm}|m \in [1, M]\}_v$ as a more interpretable and orderly mixture of Gaussian distributions, which involves altering the original form of the $\{P_{nm}|m \in [1, M]\}_v$ distribution. This implies that we need to provide a reasonable number of components for the hypothesized distribution form of $\{P_{nm}|m \in [1, M]\}_v$, namely the mixture of Gaussian distributions, assign reasonable means and variances to these components, and provide the covariance matrices between the components. Otherwise, forced and incorrect distribution modeling approaches may detrimentally affect the accuracy of Valen's reasoning.

It is noteworthy that in the RPM problems, each instance is not only designed with problem statements, option pools, and correct option labels, but also accompanied by metadata. This metadata provides a detailed description of the progressive patterns inherent in each instance. Interestingly, the intended meaning of $\{P_{nm}|m \in [1, M]\}_v$ encoded by Valen for an RPM instance also corresponds to a progressive pattern.

Therefore, we decide to use metadata to provide relevant information about the target form of the distribution of

$\{P_{nm}|m \in [1, M]\}_v$. By enumerating all the metadata within the instances of the RPM problem, the enumerated metadata list can offer ideal information about the component centers for the target distribution form of $\{P_{nm}|m \in [1, M]\}_v$. These enumeration results are mutually independent, owing to the characteristics of metadata.

In short, we enumerate all the metadata within the instances of the RPM problem to obtain a metadata list. After processing each element in the list as a Gaussian distribution, the entire list forms a mixture of Gaussian distribution. Subsequently, we naturally assign $\{P_{nm}|m \in [1, M]\}_v$ to the corresponding component of this mixture model, thereby achieving our goal of planning the distribution of pattern representations $\{P_{nm}|m \in [1, M]\}_v$. This process can be visualized as Figure 19. In the figure 19, it can be seen that we assume

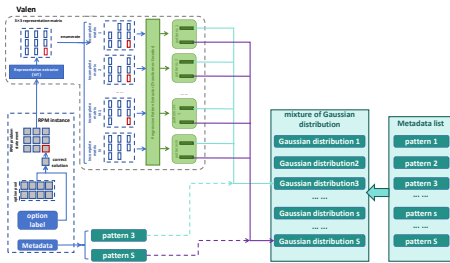


Fig. 19. The framework of SBR

the number of elements in the metadata list to be S . Since there are often multiple decoupled progressive patterns within the RPM matrix, such as the “shape” and “line” progressive patterns present in the PGM problem [16], and the related metadata fully describes these progressive patterns, we decide to dissect all the progressive patterns recorded in the metadata and use them to individually guide the assignment of the M progressive patterns stored in the $\{P_{nm}|m \in [1, M]\}_v$ to their respective distribution components. In the figure, we dissect the two progressive patterns, “pattern 3” and “pattern S”, recorded in the metadata and use them separately to guide the distribution attribution of $\{P_{n1}|n \in [1, 9]\}_v$ and $\{P_{n2}|n \in [1, 9]\}_v$. Evidently, when Valen is combined with the SBR method, the value of M is no longer an arbitrarily set hyperparameter, but rather needs to be determined based on the types of decoupled progressive patterns stored in the metadata. For example, when the SBR method is applied to the PGM problem, the value of M in Valen needs to be set to 2.

Regarding how we process each element in the enumerated metadata list into distributions, we choose to use a standard Transformer-Encoder to encode the elements, which are descriptions of the progressive patterns, into vectors directly. A list containing S elements will be encoded into S vectors, which we denote as $\{q_s|s \in [1, S]\}$ here. If the first half of q_s is regarded as the mean of a Gaussian distribution and the second half as the logarithm of variance, then $\{q_s|s \in [1, S]\}$ can represent a mixture of Gaussian distributions. We can again utilize the reparameterization technique shown in Figure 14 to reparameterize $\{q_s|s \in [1, S]\}$ into a new set of vectors, which we denote as $\{Q_{st}|s \in [1, S], t \in [1, T]\}$.

In $\{Q_{st}|s \in [1, S], t \in [1, T]\}$, it can be observed that we reparameterized $\{q_s|s \in [1, S]\}$ T times, where T is set to 10 in this paper.

Regarding the process indicated by the light blue and purple lines in the figure 19, where $\{P_{n1}|n \in [1, 9]\}_v$ and $\{P_{n2}|n \in [1, 9]\}_v$ are separately compressed into the corresponding Gaussian distribution q_3 and q_5 , we achieve this by setting an additional loss function. This loss function can be expressed as follows:

$$\begin{aligned} \{\bar{P}_{nm}\} &= \frac{1}{V} \sum_{v=1}^V \{P_{nm}\}_v \quad (5) \\ \ell_{\text{SBR}} &= - \sum_{m=1}^M \sum_{\tilde{s}=1}^S \sum_{n=1}^9 \sum_{t=1}^T \text{meta}_{m\tilde{s}} \cdot \log \frac{e^{(\bar{P}_{nm} \cdot Q_{\tilde{s}t})/\tau}}{\sum_{s=1}^S e^{(\bar{P}_{nm} \cdot Q_{st})/\tau}} \quad (6) \end{aligned}$$

Where $\text{meta}_{m\tilde{s}}$ represents whether the the m -th progressive pattern recorded in the metadata of current instance matches the \tilde{s} -th element in the metadata list and τ is a learnable parameter. As can be seen from the formula (5), considering the overhead of computational resources, we do not individually compress each viewpoint in $\{P_{nm}|n \in [1, 9], m \in [1, M]\}_v$ into the constructed mixture of Gaussian distributions, but instead first calculate the viewpoint average $\{\bar{P}_{nm}|n \in [1, 9], m \in [1, M]\}$ of $\{P_{nm}|n \in [1, 9], m \in [1, M]\}_v$ and then plan the distribution of $\{\bar{P}_{nm}|n \in [1, 9], m \in [1, M]\}$.

Formula (5) has clearly elucidated the mechanism of SBR. SBR calculates the probability of each of the M pattern representations in $\{P_{nm}|n \in [1, 9], m \in [1, M]\}$ belonging to every component in the mixture of Gaussian distributions $\{q_s|s \in [1, S]\}$, thereby obtaining $M \times S$ probability values. Subsequently, SBR applies the CE loss to constrain the $M \times S$ probabilities according to the indications of metadata. These $M \times S$ probabilities are obtained by calculating the sample cosine distance between $\{\bar{P}_{nm}|n \in [1, 9], m \in [1, M]\}$ and $\{Q_{st}|s \in [1, S], t \in [1, T]\}$, and normalizing these distances through the softmax function.

Unfortunately, the descriptions of clustering patterns in Bongard-Logo are overly simplistic, rendering the SBR a specialized solution tailored specifically for RPM problems.

VIII. EXPERIMENT

All experiments were programmed in Python using the PyTorch [41] framework.

A. Experiment on RAVEN

Initially, we tested Valen on RAVEN and I-RAVEN datasets to show its potential. For a fair comparison, we used the same settings and equipment as RS-Tran [28] and Triple-CFN [32], including data volume, optimizer parameters, data augmentation, batch size, and other hyperparameters.

The experimental records in Table I demonstrate that existing excellent RPM solvers, including Valen, exhibit varying reasoning accuracy on the RAVEN [15] and I-RAVEN [34] datasets. The I-RAVEN dataset was designed to address limitations in the RAVEN’s option pool by enhancing its negative sample setup, such as increasing the number of attributes with

TABLE I
REASONING ACCURACIES ON RAVEN AND I-RAVEN.

Model	Test Accuracy(%)							
	Average	Center	2 × 2 Grid	3 × 3 Grid	L-R	U-D	O-IC	O-IG
SAVIR-T [24]	94.0/98.1	97.8/99.5	94.7/98.1	83.8/93.8	97.8/99.6	98.2/99.1	97.6/99.5	88.0/97.2
SCL [23], [24]	91.6/95.0	98.1/99.0	91.0/96.2	82.5/89.5	96.8/97.9	96.5/97.1	96.0/97.6	80.1/87.7
MRNet [21]	96.6/-	-/-	-/-	-/-	-/-	-/-	-/-	-/-
RS-TRAN [28]	98.4/98.7	99.8/100.0	99.7/99.3	95.4/96.7	99.2/100.0	99.4/99.7	99.9/99.9	95.4/95.4
Triple-CFN [32]	98.9/99.1	100.0/100.0	99.7/99.8	96.2/97.5	99.8/99.9	99.8/99.9	99.9/99.9	97.0/97.3
Triple-CFN+Re-space [32]	99.4/99.6	100.0/100.0	99.7/99.8	98.0/99.1	99.9/100.0	99.9/100.0	99.9/99.9	98.5/99.0
Valen	99.5/99.7	100.0/100.0	99.7/99.8	98.2/99.2	99.9/100.0	99.9/100.0	99.9/99.9	98.8/99.2

shifts and the magnitude of attribute shifts. However, these modifications did not alter the configuration of the primary samples or the distribution of correct solutions. Nonetheless, the same solvers still achieved different reasoning accuracies on RAVEN and I-RAVEN. This observation aligns with our perspective in Tine: the learning objective of probabilistic highlighting solvers is not the distribution of correct solutions, but rather the distribution delineated by both primary and auxiliary samples.

B. Experiment on Bongard-Logo

We conducted experiments on Bongard-Logo. The experimental results are presented in the table II. Observing table II,

TABLE II
REASONING ACCURACIES OF MODELS ON BONGARD-LOGO.

Model	Accuracy(%)				
	Train	FF	BA	CM	NV
MetaOptNet	75.9	60.3	71.6	65.9	67.5
ANIL	69.7	56.6	59.0	59.6	61.0
Meta-Baseline-SC	75.4	66.3	73.3	63.5	63.9
Meta-Baseline-MoCo [39]	81.2	65.9	72.2	63.9	64.7
WReN-Bongard	78.7	50.1	50.9	53.8	54.3
SBSD	83.7	75.2	91.5	71.0	74.1
PMoC	92.0	90.6	97.7	77.3	76.0
Triple-CFN	93.2	92.0	98.2	78.0	78.1
Valen	92.5	91.0	97.8	77.5	76.5
Valen+Tine	93.3	92.4	98.2	78.0	77.8
Funny+Valen	95.1	93.4	98.8	80.3	79.8
Funny+Valen+Tine	96.0	95.2	99.6	84.6	82.9

The performance of Funny, Valen and Tine were promising.

C. Experiment on PGM

In this paper, we conducted experiments related to Valen on PGM. And the results are recorded in Tabel III.

From the table III, it can be observed that the SBR, Tine, and Funny methods have all contributed to varying degrees of improvement in Valen’s performance on RPM problems. Valen combined with the Funny method is the first to achieve a reasoning accuracy exceeding 99.0% on the PGM problem without relying on any additional supervisory signals. Furthermore, the integration of SBR with Valen is the

TABLE III
REASONING ACCURACIES OF MODELS ON PGM.

Model	Test Accuracy(%)
SAVIR-T [24]	91.2
SCL [23], [24]	88.9
MRNet [21]	94.5
RS-CNN [28]	82.8
RS-TRAN [28]	97.5
Triple-CFN [32]	97.8
Triple-CFN+Re-space layer [32]	98.2
Valen	98.5
Valen+Tine	98.8
Funny+Valen	99.0
RS-Tran+Tranclip [28]	99.0
Meta Triple-CFN [32]	98.4
Meta Triple-CFN+Re-space layer [32]	99.3
SBR+Valen	99.4

first approach to utilize metadata as an additional supervisory signal, achieving a reasoning accuracy of 99.4%. Additionally, SBR provides Valen with interpretability by endowing it with a progressive pattern extraction process. The SBR method presented in this paper is not the first to consider utilizing the accompanying metadata within RPM problem instances to assist the solver in reasoning. Previous works [21] have explored various approaches to leveraging metadata, but they ultimately found that forcibly imposing additional metadata learning tasks on their solvers was counterproductive. RS-Tran [28] and Triple-CFN [28] adopted an indirect manner of utilizing metadata. Specifically, RS-Tran utilizes Tranclip [28] to pre-train its representation encoder using metadata, and Triple-CFN required a similar warm-start process. However, the SBR method in this paper is the first to directly utilize metadata to model the distribution of progressive pattern representations, which is an unexplored approach in previous works and has achieved promising results.

We also conducted experiments on the interpolation and extrapolation problems in PGM, and the results are recorded in Table IV. As can be seen from the table IV, the Funny method brings a remarkable improvement to Valen in interpolation.

TABLE IV
GENERALIZATION RESULTS OF VALEN IN PGM.

Dataset	Accuracy(%)			
	Valen	Valen+Tine	Funny+Valen	SBR+Valen
Interpolation	81.2	82.8	87.6	92.5
Extrapolation	18.4	18.5	18.5	12.8

IX. CONCLUSION

In conclusion, this paper introduces a novel baseline model, Valen, for solving visual abstract reasoning tasks, particularly Bongard-Logo problems and RPM problems. Valen,

a probabilistic-highlighting model, demonstrates remarkable performance in handling both image clustering reasoning and image progression pattern reasoning. The paper further delves into the underlying mechanisms of probability-highlighting solvers, realizing that these solvers approximate solutions to reasoning problem instances as distributions. To bridge the discrepancies between the estimated solution distribution and the true correct solution distribution, the paper introduces three methods: Tine, Funny, and SBR. The Tine method, based on adversarial learning, aims to assist Valen in estimating a solution distribution closer to the correct one. The Funny method models the sample distribution within reasoning problems as a mixture of Gaussian distributions, enabling Valen to more directly capture the true form of the correct solution distribution. The SBR method further extends this idea by modeling the distribution of progressive patterns representation as a mixture of Gaussian distributions. This paper demonstrates the importance of explicitly planning the distribution of solutions in solving visual abstract reasoning problems through the successful application of the SBR, Funny, Valen and Tine.

REFERENCES

- [1] Deng, J., Dong, W., Socher, R., Li, L. J., Li, K., & Fei-Fei, L. Imagenet: A large-scale hierarchical image database. In IEEE Conference on Computer Vision and Pattern Recognition, 246-255 (2009).
- [2] Krizhevsky, A., Sutskever, I., & Hinton, G. E. Imagenet classification with deep convolutional neural networks. *Communications of the ACM*, 60(6), 84-90 (2017).
- [3] He, K., Zhang, X., Ren, S., & Sun, J. Deep Residual Learning for Image Recognition. In IEEE Conference on Computer Vision and Pattern Recognition, 770-778 (2016).
- [4] Vaswani, A. *et al.* Attention is All You Need. In *Advances in Neural Information Processing Systems*, (2017).
- [5] Devlin, J., Chang, M. W., Lee, K., & Toutanova, K. Bert: Pre-training of Deep Bidirectional Transformers for Language Understanding. Preprint at <https://arxiv.org/abs/1810.04805> (2018).
- [6] Brown, T. *et al.* Language Models are Few-shot Learners. In *Advances in Neural Information Processing Systems*, 1877-1901 (2020).
- [7] Goodfellow, I. *et al.* Generative adversarial networks. *Communications of the ACM*, 63(11), 139-144 (2020).
- [8] Kingma, D. P., & Welling, M. Auto-encoding variational bayes. Preprint at <https://arxiv.org/abs/1312.6114> (2014).
- [9] Ho, J., Jain, A., & Abbeel, P. Denoising diffusion probabilistic models. In *Advances in Neural Information Processing Systems*, 33, 6840-6851 (2020).
- [10] Antol, S., Agrawal, A., Lu, J., Mitchell, M., Batra, D., Zitnick, C. L., & Parikh, D. VQA: Visual question answering. In IEEE International Conference on Computer Vision, 2425-2433 (2015).
- [11] Johnson, J., Hariharan, B., Van Der Maaten, L., Fei-Fei, L., Lawrence Zitnick, C., & Girshick, R. Girshick. CLEVR: A Diagnostic Dataset for Compositional Language and Elementary Visual Reasoning. In IEEE Conference on Computer Vision and Pattern Recognition, 2901-2910 (2017).
- [12] Depeweg, S., Rothkopf, C. A., & Jäkel, F. Solving Bongard Problems with a Visual Language and Pragmatic Reasoning. Preprint at <https://arxiv.org/abs/1804.04452> (2018).
- [13] Nie, W., Yu, Z., Mao, L., Patel, A. B., Zhu, Y., & Anandkumar, A. Bongard-Logo: A New Benchmark for Human-Level Concept Learning and Reasoning. In *Advances in Neural Information Processing Systems*, 16468-16480 (2020).
- [14] Raven J. C. Raven's Progressive Matrices. (Western Psychological Services, (1938).
- [15] Zhang, C., Gao, F., Jia, B., Zhu, Y., & Zhu, S. C. Raven: A Dataset for Relational and Analogical Visual Reasoning. In Proceedings of the IEEE/CVF Conference on Computer Vision and Pattern Recognition, 5317-5327 (2019).
- [16] Barrett, D., Hill, F., Santoro, A., Morcos, A., & Lillicrap, T. Measuring Abstract Reasoning in Neural Networks. In International Conference on Machine Learning, 511-520 (2018).
- [17] Dosovitskiy, A. *et al.* An Image is Worth 16x16 Words: Transformers for Image Recognition at Scale. Preprint at <https://arxiv.org/abs/2010.11929> (2020).
- [18] Zheng, K., Zha, Z. J., & Wei, W. Abstract Reasoning with Distracting Features. In *Advances in Neural Information Processing Systems*, (2019).
- [19] Zhang, C., Jia, B., Gao, F., Zhu, Y., Lu, H., & Zhu, S. C. Learning Perceptual Inference by Contrasting. In Proceedings of Advances in Neural Information Processing Systems, (2019).
- [20] Zhuo, T., & Kankanhalli, M. Effective Abstract Reasoning with Dual-Contrast Network. In Proceedings of International Conference on Learning Representations, (2020).
- [21] Benny, Y., Pekar, N., & Wolf, L. Scale-Localized Abstract Reasoning. In Proceedings of the IEEE/CVF Conference on Computer Vision and Pattern Recognition, 12557-12565, (2021).
- [22] Zhuo, Tao and Huang, Qiang & Kankanhalli, Mohan. Unsupervised abstract reasoning for raven's problem matrices. *IEEE Transactions on Image Processing*, 8332-8341, (2021).
- [23] Wu, Y., Dong, H., Grosse, R., & Ba, J. The Scattering Compositional Learner: Discovering Objects, Attributes, Relationships in Analogical Reasoning. Preprint at <https://arxiv.org/abs/2007.04212> (2020).
- [24] Sahu, P., Basioti, K., & Pavlovic, V. SAViR-T: Spatially Attentive Visual Reasoning with Transformers. Preprint at <https://arxiv.org/abs/2206.09265> (2022).
- [25] Zhang, C., Jia, B., Zhu, S. C., & Zhu, Y. Abstract Spatial-Temporal Reasoning via Probabilistic Abduction and Execution. In Proceedings of the IEEE/CVF Conference on Computer Vision and Pattern Recognition, 9736-9746 (2021).
- [26] Zhang, C., Xie, S., Jia, B., Wu, Y. N., Zhu, S. C., & Zhu, Y. Learning Algebraic Representation for Systematic Generalization. In Proceedings of the European Conference on Computer Vision, (2022).
- [27] Hersche, M., Zeqiri, M., Benini, L., Sebastian, A., & Rahimi, A. A Neuro-vector-symbolic Architecture for Solving Raven's Progressive Matrices. Preprint at <https://arxiv.org/abs/2203.04571> (2022).
- [28] Q. Wei, D. Chen, B. Yuan, Multi-viewpoint and multi-evaluation with felicitous inductive bias boost machine abstract reasoning ability, *arXiv* :2210.14914, 2022.
- [29] Shi, Fan, Bin Li, and Xangyang Xue. "Abstracting Concept-Changing Rules for Solving Raven's Progressive Matrix Problems." *arXiv preprint arXiv:2307.07734* (2023).
- [30] S.Kharagorgiev,"Solvingbongardproblemswithdeeplearning," [k10v.github.io](https://github.com/k10v),2020.
- [31] R.Song, B.Yuan. Solving the bongard-Logo problem by modeling a probabilistic model. Preprint at <https://arxiv.org/abs/> *arXiv:2403.03173* (2024).
- [32] R.Song, B.Yuan. Triple-CFN: Restructuring Concept Spaces for Enhancing Abstract Reasoning process. Preprint at <https://arxiv.org/abs/arXiv:2403.03190> (2024).
- [33] Arjovsky, Martin, Soumith Chintala, and Léon Bottou. "Wasserstein generative adversarial networks." International conference on machine learning. PMLR, 2017.
- [34] Hu, S., Ma, Y., Liu, X., Wei, Y., & Bai, S. Stratified Rule-Aware Network for Abstract Visual Reasoning. In Proceedings of the AAAI Conference on Artificial Intelligence, 1567-1574 (2021).
- [35] Zhuo, T., Huang, Q., & Kankanhalli, M. Unsupervised Abstract Reasoning for Raven's Problem Matrices. *IEEE Transactions on Image Processing*, 8332 - 8341 (2021).
- [36] Carpenter, P. A., Just, M. A., & Shell, P. What One Intelligence Test Measures: a Theoretical Account of the Processing in the Raven Progressive Matrices Test. *Psychological review*, 97(3), 404, (1990).
- [37] Bardes, Adrien, Jean Ponce, and Yann LeCun. "Vicreg: Variance-invariance-covariance regularization for self-supervised learning." *ar**v preprint ar**v:2105.04906* (2021).
- [38] Oord, A. V. D., Li, Y., & Vinyals, O. Representation Learning with Contrastive Predictive Coding. Preprint at <https://arxiv.org/abs/1807.03748> (2019).
- [39] He, K., Fan, H., Wu, Y., Xie, S., & Girshick, R. Momentum Contrast for Unsupervised Visual Representation Learning. In Proceedings of the IEEE/CVF Conference on Computer Vision and Pattern Recognition, 9729-9738 (2020).
- [40] Locatello, Francesco, et al. "Challenging common assumptions in the unsupervised learning of disentangled representations." international conference on machine learning. PMLR, 2019.
- [41] Paszke, A. *et al.* Automatic Differentiation in Pytorch. In NIPS Autodiff Workshop. (2017).